Middle East Journal of Applied Sciences
Volume: 16 | Issue: 01| Jan. – Mar. | 2026

EISSN: 2706 -7947 ISSN: 2077- 4613
DOI: 10.36632/mejas/2026.16.1.5
Journal homepage: www.curresweb.com
Pages: 54-80

Distribution and Mineralogical Evaluation of Heavy Minerals in Three-Meter Subsurface Coastal Sediments of the Baltim–El Burullus Area, Egypt

Mansur S. M.[1], Hassan M. H.[2], Khalifa I. H.[3], El-Azab A.I.[1] and Seif R. A.[4]

[1]Nuclear Materials Authority, Egypt.
[2]Ahram Canadian University, Egypt.
[3]Geology Department, Faculty of Science, Suez Canal University, Egypt.
[4]Geology Department, Faculty of Science, Suez Canal University, Egypt.

Received: 20 Jan. 2026 **Accepted:** 15 Mar. 2026 **Published:** 30 Mar. 2026

ABSTRACT

This study focuses on the mineralogical investigation of heavy minerals distributed within the coastal sediments of the Baltim–El Burullus area along the northern Mediterranean coast of Egypt. A total of 60 sediment samples were collected from 20 boreholes drilled to a depth of 3 meters, where one representative sample was obtained from each meter interval. The collected samples were processed using heavy liquid separation techniques, including bromoform, methylene iodide, and Clerici's solution, followed by detailed examination under a binocular stereomicroscope and ESEM–EDX analyses. The investigated sediments contain a variety of economically important heavy minerals, mainly magnetite, ilmenite, rutile, leucoxene, garnet, zircon, and monazite, in addition to minor accessory minerals such as apatite, titanite, and staurolite. The results show that ilmenite is the most abundant heavy mineral, with concentrations ranging from 1.701% to 16.791% and an average value of 6.033%. Magnetite contents range between 0.015% and 1.165%, averaging 0.19%, while garnet concentrations vary from 0.55% to 2.522% with an average of 1.20%. Zircon contents range from 0.05% to 1.337% with an average of 0.497%, whereas rutile ranges between 0.064% and 1.031% with an average of 0.269%. Leucoxene concentrations vary from 0.102% to 0.919% with an average of 0.448%, while monazite occurs in relatively low amounts ranging from 0% to 0.787%, with an average value of 0.034%. The vertical distribution of heavy minerals indicates a noticeable decrease in mineral concentrations with increasing depth, reflecting the influence of sedimentary and hydrodynamic processes on the accumulation of black sand minerals in the study area. The obtained results confirm the economic importance of the Baltim–El Burullus coastal sediments as a potential source of valuable heavy minerals and provide essential mineralogical information that may support future exploitation and environmental evaluation of these coastal deposits.

Keywords: Heavy minerals, Black sand deposits, Baltim El Burullus, Coastal sediments, Mineralogical investigation, Ilmenite, Magnetite, Zircon, Monazite, Heavy liquid separation, ESEM–EDX analysis, Mediterranean coast of Egypt, Borehole sediments, Sedimentology, Economic minerals.

Introduction

Mechanical processes represent an important means for forming mineral deposits called placers through gravity concentration of weathering-resistant materials. The quantity and variety of resistant minerals in placer deposits are a function of the source rocks, the types and intensity of weathering, selective sorting during transportation and deposition, and subsequent reworking of the sediments after deposition (Basu and Molinaroli, 1989; Bryan *et al*., 2007; Mc-Lemore, 2010). Large deposits of potentially economic heavy minerals occur along the recent shoreline of the Nile Delta and Sinai, in a zone extending from Rafah in the east to Abu Qir in the west, where heavy minerals are found in beach sands, sand dunes, and sandbars such as Idku, El-Burullus, El-Manzala, and El-Bardawil, which are

Corresponding Author: Hassan M. H., Ahram Canadian University, Egypt.
E-mail: hassan31mohamed@icloud.com

considered natural mineral traps. Ball (1907) reported the first observation of heavy minerals in the Nile sediments, and later Hume (1925) noted that a streak of black heavy minerals is restricted to the water line on the sand bank along the Nile River, also observing higher specific gravity of beach sand compared to inland sands. Despite these early observations, the Egyptian black sands on the coastal plain of the Nile Delta were only exploited in the 1940s, with academic and applied studies beginning later with the mineralogical work of Shukri (1950), while most subsurface investigations were conducted on the east Rashid beach due to high surface concentrations of heavy minerals. The mineral assemblages of Egyptian black sands have long been recognized as reliable indicators for understanding the evolution of coastal environments and sedimentary processes. These deposits are not only important from a geological perspective but also represent a strategic source of raw materials required for several industrial sectors, including nuclear, metallurgical, and engineering applications. Among the economic minerals, opaque minerals are the most abundant, forming nearly 86% of the total economic heavy mineral content (Dabbour, 1995). According to Anwar and El-Bouseily (1970), these opaque grains consist predominantly of iron oxide minerals, which play a major role in determining the economic value of the black sand deposits. (1973) identifying them as magnetite, ilmenite, and hematite. The heavy minerals in the study area are mainly magnetite, ilmenite, garnet, leucoxene, rutile, zircon, and monazite, which are potentially economic, while hematite, apatite, staurolite, and titanite occur as accessory minerals.

The present work is concerned with the distribution of heavy minerals along the coastal plain of the Mediterranean Sea limited by Burg El Burullus town to the west and El Gharbia outlet to the east, and in this study, the evaluation of concentrations of heavy minerals in both beach and sabkha sediments along the Baltim-El Burullus coastal sector were investigated. To perform this work, the collected samples were subjected to heavy liquid separation and detailed microscopic studies using different techniques. The distribution of economic heavy minerals on the beach and coastal plain is of great importance for mining developments of these deposits and for environmental management of the coastal zone.

Mineralogy

Sampling and Preparation

Sixty sediment samples were collected from 20 locations along the study area. At each location, a borehole reaching a depth of 3 m was drilled using a mechanical drilling machine, and one representative sample was collected from each meter, resulting in a total of 60 sediment samples. The collected samples were air-dried and prepared for mineral separation through heavy liquid techniques based on differences in specific gravity among mineral constituents. Initially, bromoform solution (specific gravity: 2.86 g/cm³) was used to separate light minerals, such as quartz and feldspars, from the heavy mineral fraction. In addition, methylene iodide (specific gravity: 3.6 g/cm³) and Clerici's solution (specific gravity: 4.01 g/cm³) were applied to isolate minerals with higher specific gravities, particularly the ultra-heavy mineral assemblages.

Each sample was placed in a separating funnel containing the heavy liquid and thoroughly stirred before being allowed to settle into two distinct layers. The upper floating layer consisted mainly of light minerals, including quartz, feldspars, calcite, and mica flakes, whereas the lower sink layer represented the heavy mineral fraction. The heavy fractions were collected using filter paper, washed carefully with acetone to remove residual heavy liquids, dried, weighed, and their weight percentages were calculated and presented in Table (1). The separated heavy mineral concentrates were selected for further analytical work, while the lighter sediment fractions were considered non-essential and therefore omitted from subsequent investigations.

A preliminary magnetic separation was performed to remove magnetite from the heavy mineral concentrate using a hand magnet of suitable strength. The recovered magnetite content was quantified and reported in Table (2). The remaining concentrate was then further subdivided into magnetic fractions using a Frantz Isodynamic Magnetic Separator (Model L-1), with operational settings of 5° side tilt and 20° forward inclination as recommended by Flinter (1955).

Microscopic examination of the separated heavy mineral assemblages under a binocular stereomicroscope indicated that the identified minerals can be categorized into two principal groups according to Folk (1980). The first group includes opaque minerals such as magnetite, hematite, ilmenite, leucoxene, and pyrite, whereas the second group comprises non-opaque minerals including

garnet, rutile, titanite, zircon, monazite, and apatite. Less stable minerals, including kyanite, sillimanite, andalusite, epidote, biotite, muscovite, and green silicates, were also recognized. The relative percentages of each mineral within the total heavy mineral assemblage, together with the ranges and average values of total heavy minerals in the studied sediments, were calculated and summarized in Table (3).

Mineralogical characterization of the identified mineral constituents was further supported by semi-quantitative EDX chemical analyses performed on selected heavy mineral grains using a Phillips XL-30 Environmental Scanning Electron Microscope (ESEM). The most economically and environmentally significant heavy minerals identified in the studied sediments are discussed in the following sections.

Table 1: The Percentages of heavy bromoform, methylene, and clerici's of the studied sediments**.**

S. No.	First Meter			Second Meter			Third Meter		
	H.Br. %	H.MI. %	H. Cl.%	H.Br. %	H.MI. %	H.Cl. %	H.Br. %	H.MI. %	H.Cl. %
1	28.814	20.538	8.276	20.668	15.57	5.098	18.458	13.652	4.806
2	37.981	27.112	10.869	22.594	16.5	6.094	17.667	12.808	4.859
3	30.576	22.349	8.227	24.84	18.343	6.497	17.729	13.486	4.243
4	26.923	20.675	6.248	21.984	16.899	5.085	17.581	13.334	4.247
5	31.451	21.529	9.922	20.771	15.852	4.919	15.474	12.197	3.277
6	33.677	22.845	10.832	22.539	16.883	5.656	21.559	15.528	6.031
7	36.414	24.466	11.948	20.723	15.367	5.356	20.838	14.675	6.163
8	27.115	19.479	7.636	23.338	17.364	5.974	17.938	13.557	4.381
9	33.192	23.69	9.502	21.576	16.287	5.289	13.49	11.782	1.708
10	53.648	37.013	16.635	19.614	15.085	4.529	16.376	12.302	4.074
11	41.799	28.975	12.824	24.242	17.588	6.654	15.62	11.912	3.708
12	38.238	26.819	11.419	25.075	17.892	7.183	16.554	12.83	3.724
13	36.126	25.804	10.322	22.712	17.097	5.615	16.827	12.462	4.365
14	33.875	24.337	9.538	22.54	16.811	5.729	16.181	12.213	3.968
15	29.158	20.966	8.192	26.11	18.486	7.624	18.972	14.292	4.68
16	29.363	21.257	8.106	23.475	16.501	6.974	17.653	13.206	4.447
17	32.779	23.909	8.87	23.965	16.692	7.273	16.829	12.513	4.316
18	38.066	25.72	12.346	23.688	16.849	6.839	12.135	10.026	2.109
19	42.836	29.937	12.899	24.649	17.981	6.668	17.154	12.238	4.916
20	44.151	30.773	13.378	26.454	18.952	7.502	21.793	15.537	6.256
Min.	25.727	19.479	6.248	19.614	15.085	4.529	12.135	10.026	1.708
Max.	53.648	37.013	16.635	26.576	18.952	7.624	21.793	15.537	6.256
Ave.	35.308	24.909	10.399	23.077	16.949	6.128	17.342	13.028	4.314

S. No. = Sample Number HBr. % = Heavy Bromoform HMi. % = Heavy Methylene HCl. % = Heavy clerici's Min. = Minimum Max. = Maximum Ave. = Average

Table 2: The distribution percentage of heavy minerals in the studied sediments.

S. No.	Depth	Mg. %	Ilm. %	Gar. %	Leuc. %	Mon. %	Zir. %	Rut. %	GS. %	Sum %
	1	0.181	11.088	1.845	0.702	0.098	0.904	0.29	13.706	28.814
1	**2**	0.106	4.967	1.275	0.702	0.026	0.583	0.2	12.809	20.668
	3	0.103	5.705	1.2	0.349	0.043	0.677	0.186	10.195	18.458
	1	0.1	10.601	1.919	0.919	0.083	0.083	1.031	23.245	37.981
2	**2**	0.147	5.377	1.122	0.464	0.033	0.519	0.25	14.682	22.594
	3	0.139	3.468	0.975	0.359	0	0.338	0.121	12.267	17.667
	1	0.053	5.2	2.191	0.864	0.787	0.05	0.911	20.52	30.576
3	**2**	0.16	4.791	1.993	0.734	0.085	0.584	0.183	16.31	24.84
	3	0.062	3.645	0.795	0.32	0.002	0.437	0.126	12.342	17.729
	1	0.138	6.797	1.325	0.734	0.075	0.673	0.306	16.875	26.923
4	**2**	0.132	4.579	1.31	0.613	0.029	0.638	0.207	14.476	21.984
	3	0.124	4.633	1.077	0.265	0.025	0.355	0.226	10.876	17.581
	1	0.192	7.976	1.832	0.627	0.005	0.826	0.389	19.604	31.451
5	**2**	0.117	4.95	1.659	0.431	0.007	0.156	0.391	13.06	20.771
	3	0.091	2.43	0.786	0.291	0.014	0.322	0.067	11.473	15.474
	1	0.214	8.587	2.363	0.646	0.021	0.383	0.839	20.624	33.677
6	**2**	0.113	4.842	1.011	0.543	0.002	0.28	0.235	15.513	22.539
	3	0.123	5.245	0.854	0.128	0.001	0.447	0.208	14.553	21.559
	1	1.165	8.851	1.868	0.655	0.031	0.693	0.397	22.754	36.414
7	**2**	0.124	4.633	1.077	0.365	0.025	0.355	0.365	13.779	20.723
	3	0.079	4.869	0.806	0.345	0.005	0.389	0.325	14.02	20.838
	1	0.928	5.95	1.3	0.572	0.032	0.124	0.57	17.639	27.115
8	**2**	0.151	5.637	1.138	0.422	0.048	0.661	0.28	15.001	23.338
	3	0.072	4.03	0.559	0.19	0.033	0.314	0.158	12.582	17.938
	1	0.624	7.716	1.759	0.673	0.028	0.713	0.31	21.369	33.192
9	**2**	0.169	5.165	0.98	0.441	0.05	0.574	0.233	13.964	21.576
	3	0.015	2.055	0.87	0.319	0	0.109	0.09	10.032	13.49
	1	0.17	16.791	1.412	0.643	0.002	1.117	0.458	33.055	53.648
10	**2**	0.085	2.679	0.556	0.35	0.003	0.243	0.11	15.588	19.614
	3	0.051	1.701	0.616	0.208	0.037	0.207	0.064	13.492	16.376
	1	0.138	13.213	2.234	0.77	0.009	1.337	0.479	23.619	41.799
11	**2**	0.122	5.973	0.855	0.298	0.032	0.47	0.235	16.257	24.242
	3	0.085	2.482	0.8	0.221	0.002	0.188	0.153	11.689	15.62
	1	0.156	9.868	1.201	0.486	0.001	0.849	0.375	25.302	38.238
12	**2**	0.115	6.236	0.895	0.237	0.005	0.568	0.241	16.778	25.075
	3	0.018	3.485	0.712	0.102	0.006	0.279	0.128	11.824	16.554
	1	0.157	9.239	1.202	0.488	0.045	0.903	0.295	23.797	36.126
13	**2**	0.087	4.921	1.13	0.491	0.003	0.404	0.187	15.489	22.712
	3	0.559	3.048	0.672	0.326	0.004	0.344	0.146	11.728	16.827
	1	0.193	8.542	1.348	0.431	0.001	0.462	0.209	22.689	33.875
14	**2**	0.642	5.1	0.859	0.376	0.036	0.676	0.208	14.643	22.54
	3	0.175	2.988	0.58	0.208	0.017	0.311	0.125	11.777	16.181
15	**1**	0.102	7.619	0.891	0.46	0.045	0.569	0.251	19.221	29.158

	2	0.185	6.977	0.705	0.286	0.016	0.547	0.224	14.455	26.11
	3	0.18	3.941	0.895	0.237	0	0.306	0.125	13.288	18.972
	1	0.152	7.734	1.179	0.513	0.013	0.543	0.376	18.853	29.363
16	**2**	0.094	6.255	0.55	0.498	0	0.45	0.22	15.408	23.475
	3	0.095	3.008	0.725	0.366	0	0.325	0.168	12.966	17.653
	1	0.162	8.156	1.768	0.528	0.004	0.863	0.303	20.995	32.779
17	**2**	0.451	6.276	1.312	0.492	0.049	0.561	0.131	14.693	23.965
	3	0.099	3.171	0.979	0.186	0	0.256	0.122	12.016	16.829
	1	0.283	9.144	2.522	0.632	0.034	0.93	0.345	24.176	38.066
18	**2**	0.126	5.563	0.791	0.385	0	0.392	0.172	16.259	23.688
	3	0.091	2.43	0.986	0.291	0.014	0.322	0.067	7.934	12.135
	1	0.226	10.188	2.082	0.51	0.001	0.598	0.251	28.98	42.836
19	**2**	0.087	5.702	0.667	0.427	0.013	0.491	0.212	17.05	24.649
	3	0.168	4.614	0.639	0.304	0.029	0.299	0.139	10.962	17.154
	1	0.238	11.356	1.69	0.563	0.001	0.903	0.37	29.03	44.151
20	**2**	0.149	5.594	1.441	0.528	0.039	0.501	0.215	17.987	26.454
	3	0.141	4.198	1.216	0.361	0.009	0.421	0.147	15.3	21.793
Min.		0.015	1.701	0.55	0.102	0	0.05	0.064	7.934	12.135
Max.		1.165	16.791	2.522	0.919	0.787	1.337	1.031	33.055	53.648
Ave.		0.19	6.033	1.2	0.448	0.034	0.497	0.269	16.526	25.243

Economic Minerals

The opaque minerals

Magnetite (Fe_3O_4)

Magnetite (Fe_3O_4) is a ferromagnetic iron oxide composed of both ferrous and ferric ions, representing a combination of wustite and hematite, and often deviates from its theoretical composition due to magmatic differentiation and weathering processes. Egyptian black sand magnetite is characterized by heterogeneous sources and commonly contains significant amounts of titanomagnetite along with impurities such as manganese, vanadium, and chromium, which affect its industrial quality. Hammoud (1966) indicated that these impurities, along with high TiO_2 content and low magnetic susceptibility, reduce its grade for iron and steel production, whereas Nofal *et al*. (1980) demonstrated that beneficiation processes can enhance its suitability for industrial use; moreover, titanium-free magnetite constitutes only about 15 wt.% of the total (Wassef and Mikhail, 1981). Magnetite is easily separated magnetically and occurs in various forms ranging from massive to granular and angular (Fig. 1.a,b), with colors varying from black to reddish-brown due to oxidation or intergrowth with minerals such as hematite and ilmenite. These intergrowths have been widely studied (Boctor 1966; Basta 1972; Arafa 1990; Dewedar 1998; El Balakssy 2003; Hassaan 2005; Mansour 2009; Barakat 2016). Quantitative analysis shows that magnetite content varies vertically within heavy mineral fractions (Table 3), ranging from 0.053–1.165% (avg. 0.2786%) in the first meter, 0.085–0.642% (avg. 0.1681%) in the second, and 0.015–0.559% (avg. 0.1235%) in the third. ESEM and EDX analyses (Fig. 1.c–f) reveal titanium content reaching up to 16.83%, and these minerals are mainly derived from mafic volcanic rocks of the Blue Nile provenance (El-Kammar *et al*., 2010), with lateral distribution illustrated in (Fig. 2). Furthermore, a strong positive correlation between magnetite and total heavy minerals (Fig. 3) confirms that magnetite can be used as a reliable indicator for the distribution of heavy minerals under varying sedimentary conditions.

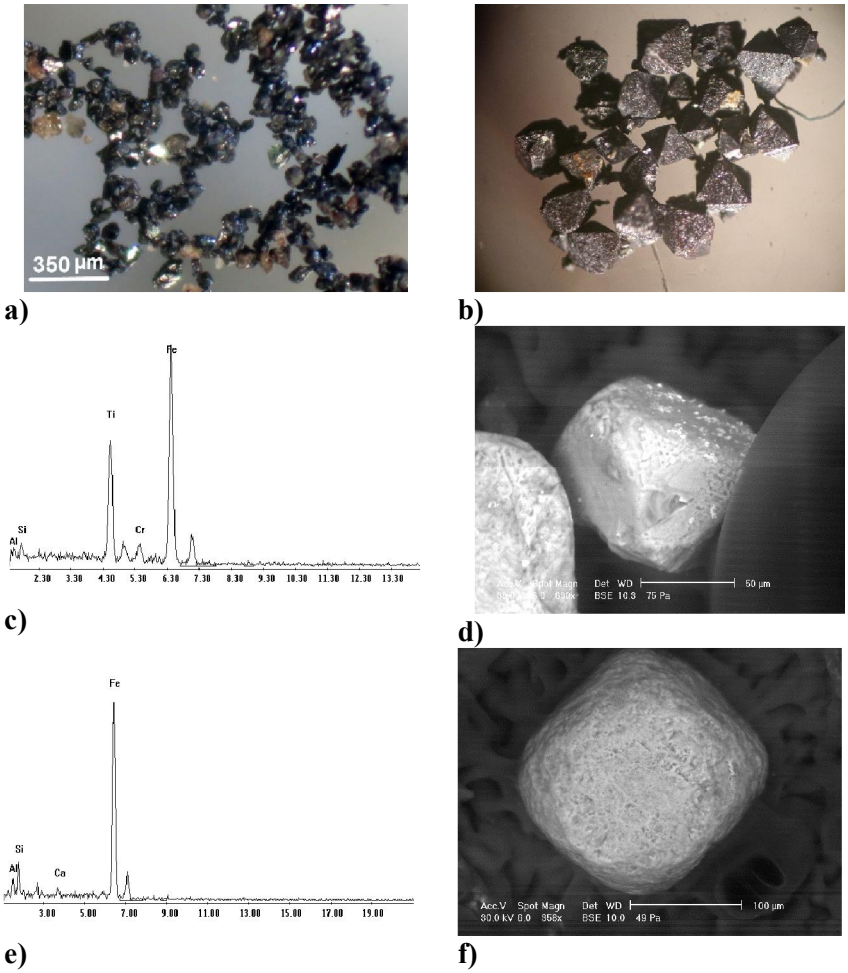

Fig. 1: Photomicrographs show: a) granular, angular to sub-angular magnetite, b) octahedron crystals of magnetite, c, d) EDX and BSE image of titano-magnetite grains and e, f) EDX and BSE image of magnetite grains.

Table 3: The Percentages of magnetite mineral in the studied samples.

S. No.	Mg. %		
	First meter	Second meter	Third meter
1	0.181	0.106	0.103
2	0.1	0.147	0.139
3	0.053	0.16	0.062
4	0.138	0.132	0.124
5	0.192	0.117	0.091
6	0.214	0.113	0.123
7	1.165	0.124	0.079
8	0.928	0.151	0.072
9	0.624	0.169	0.015
10	0.17	0.085	0.051
11	0.138	0.122	0.085
12	0.156	0.115	0.018
13	0.157	0.087	0.559
14	0.193	0.642	0.175
15	0.102	0.185	0.18
16	0.152	0.094	0.095
17	0.162	0.451	0.099
18	0.283	0.126	0.091
19	0.226	0.087	0.168
20	0.238	0.149	0.141

Min.	0.053	0.085	0.015
Max.	1.165	0.642	0.559
Ave.	0.2786	0.1681	0.1235

S. No. = Sample Number Min.=Minimum Max. =Maximum Ave.=Average

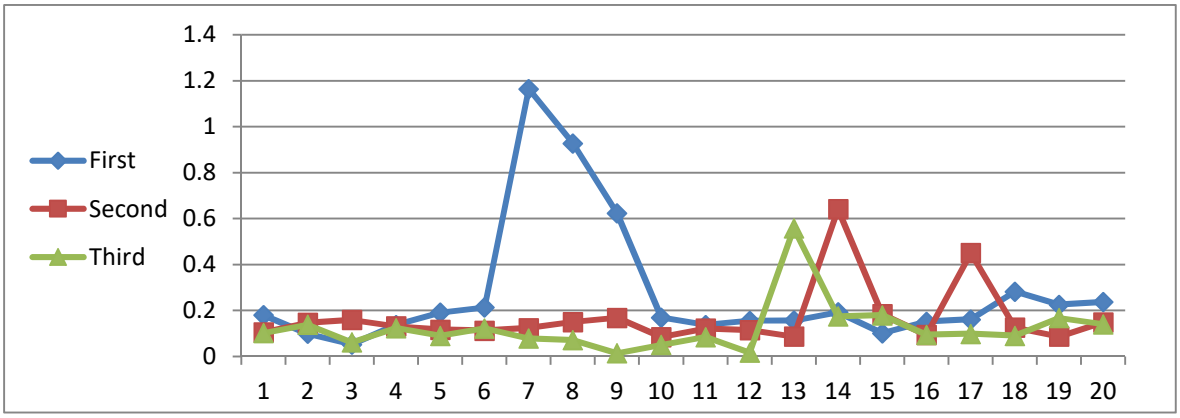

Fig. 2: Lateral distribution of magnetite in the first, second, and third meters

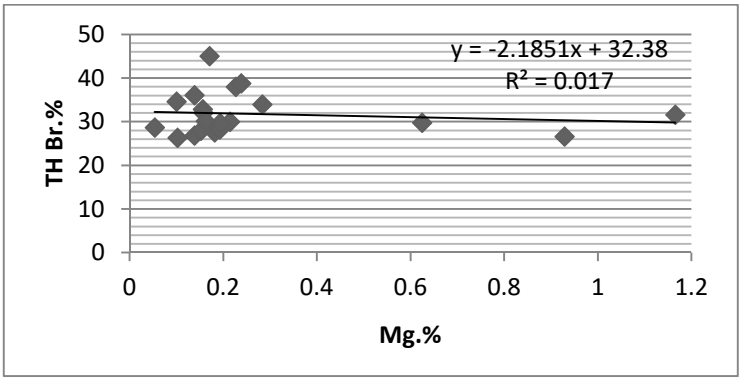

First meter

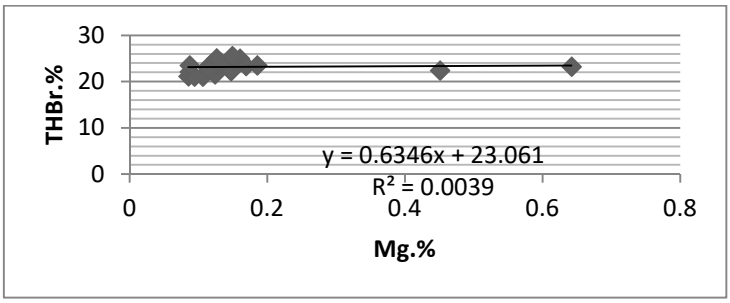

Second meter

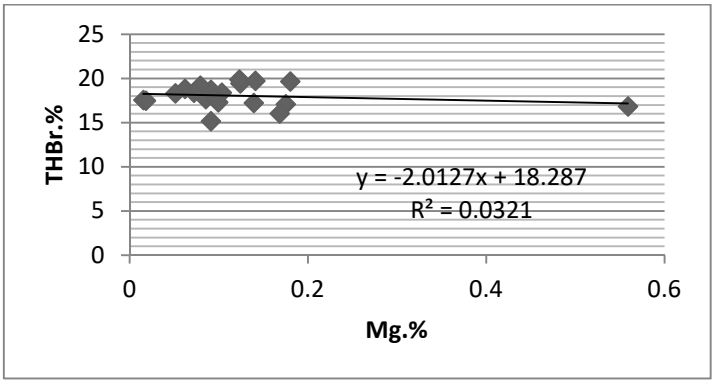

Third meter

Fig. 3: Show the relation between magnetite and the total heavy minerals in the First, Second, and Third Meter.

Ilmenite ($FeO.TiO_2$)

Ilmenite ($FeO \cdot TiO_2$) is the dominant economic heavy mineral in Egyptian black sands, constituting more than 53 wt.% of the total economic minerals. It is the most abundant Fe–Ti oxide mineral, occurring in various igneous and metamorphic rocks as well as in detrital deposits, and serves as a primary source of titanium and a secondary source of iron. Egyptian ilmenite is generally considered low-grade due to its relatively low TiO_2 content (44–48 wt.%) and higher concentrations of Fe_2O_3 and Cr_2O_3. Iron within ilmenite exists in both ferrous and ferric forms, with the ferrous form being more amenable to acid leaching; therefore, reducing ferric iron enhances extraction efficiency. Previous studies (Ramakrishnan *et al*., 1997; Eisenmann, 2001) indicate that the degree of alteration significantly influences its economic value and chemical composition, with transformations occurring between ilmenite, titaniferous hematite, and titanomagnetite, as well as exsolution textures forming at lower temperatures. Weathering processes lead to selective dissolution of hematite, enriching the remaining ilmenite in titanium. Metallurgical treatments, particularly smelting (Dawood, 2003), are recommended for Egyptian ilmenite to produce titania-rich slag (up to ~78 wt.% TiO_2) and pig iron, while beneficiation processes (Hussiny *et al*., 2008) are essential to upgrade TiO_2 content to economically viable levels (~90 wt.%). The mineral occurs in various grain shapes (Fig. 4.a–d) and is widely distributed across sediments, with vertical variations in content documented in Table (4), showing decreasing averages with depth. ESEM analysis (Fig. 4.e,f) and lateral distribution patterns (Fig. 5) further characterize its occurrence. Ilmenite and its alteration product, leucoxene, are primarily used in the production of titanium dioxide for high-quality pigments, in addition to applications in sandblasting, foundry molds, drilling fluids, anti-corrosive paints, and petroleum industry abrasives.

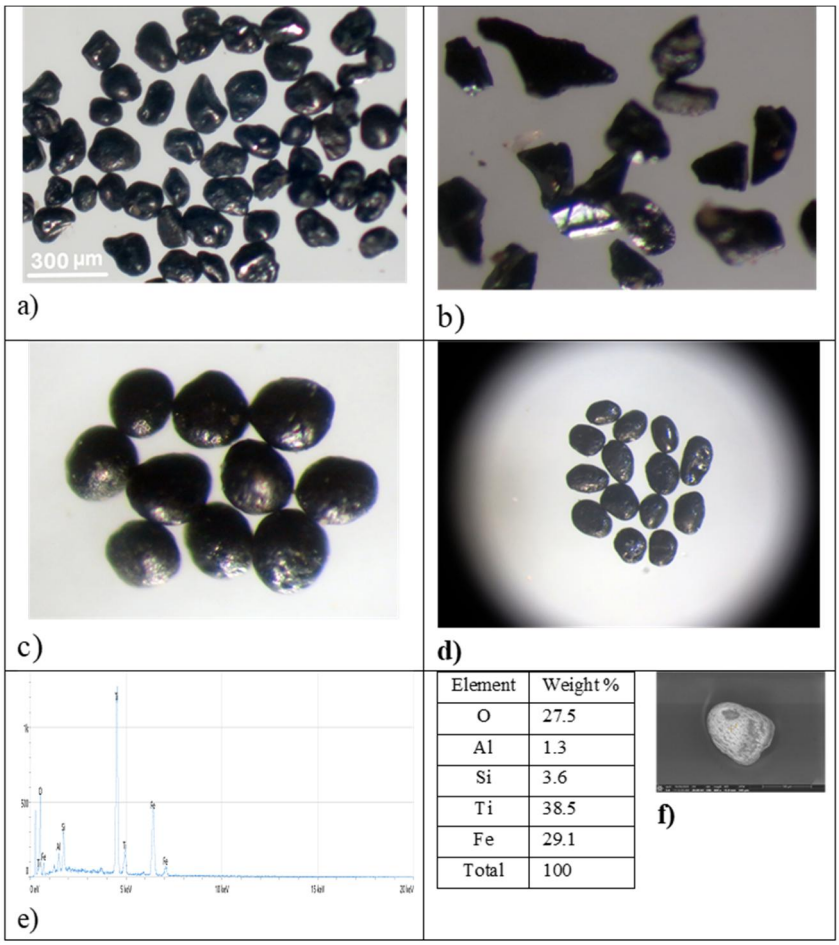

Element	Weight %
O	27.5
Al	1.3
Si	3.6
Ti	38.5
Fe	29.1
Total	100

Fig. 4: Photomicrograph shows: a) iron-black with metallic luster b) irregular ilmenite grains with sharp edges, c) well-rounded to sub-rounded with smooth edges d) oval with smooth and pitted surface e&f) EDX and BSE image of ilmenite

Table 4: The percentage of Ilmenite mineral

S. No.	Ilmenite % First Meter	Second Meter	Third Meter
1	11.088	4.967	5.705
2	10.601	5.377	3.468
3	5.2	4.791	3.645
4	6.797	4.579	4.633
5	7.976	4.95	2.43
6	8.587	4.842	5.245
7	8.851	4.633	4.869
8	5.95	5.637	4.03
9	7.716	5.165	2.055
10	16.791	2.679	1.701
11	13.213	5.973	2.482
12	9.868	6.236	3.485
13	9.239	4.921	3.048
14	8.542	5.1	2.988
15	7.619	6.977	3.941
16	7.734	6.255	3.008
17	8.156	6.276	3.171
18	9.144	5.563	2.43
19	10.188	5.702	4.614
20	11.356	5.594	4.198
Min.	5.2	2.679	1.701
Max.	16.791	6.977	5.705
Ave.	9.2308	5.31085	3.5573

S. No. = Sample Number Min.=Minimum Max. =Maximum Ave.=Average

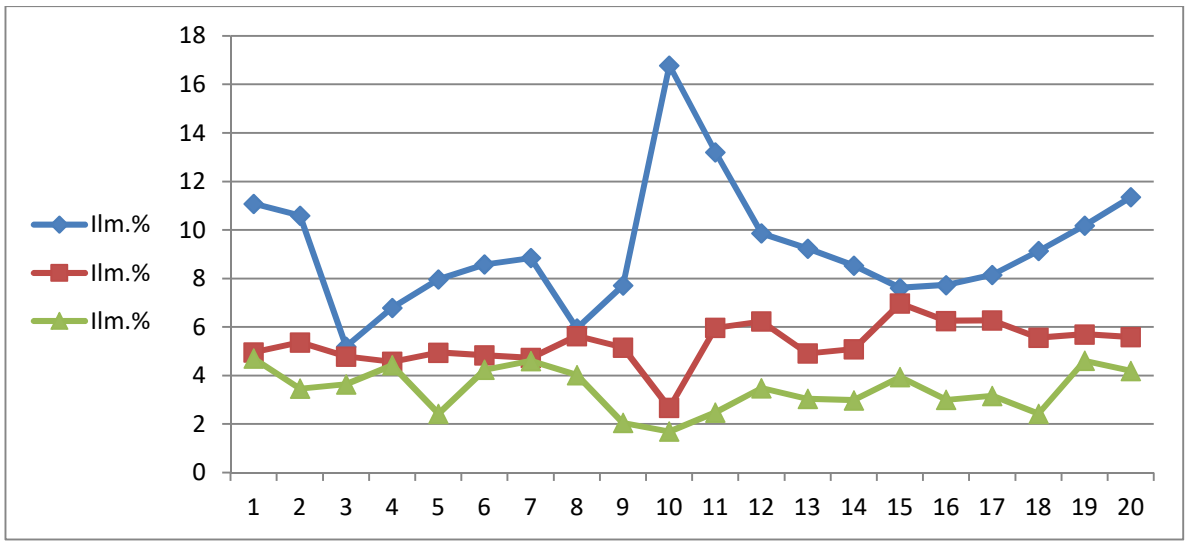

Fig. 5: Lateral distribution of ilmenite in the first, second, and third meters

Leucoxene

Leucoxene is widely recognized as an alteration product of Fe–Ti minerals, particularly ilmenite, formed through progressive weathering and chemical transformation processes (Chaudhuri and Newesely, 1990). The leucoxenization of ilmenite results in significant changes in grain color, chemical composition, internal structure, magnetic susceptibility, and specific gravity (Force, 1991), producing

a heterogeneous material typically containing more than 70 wt.% TiO_2. It represents a transitional phase between primary ilmenite and secondary rutile, and is mainly composed of fine-grained titanium oxide minerals such as brookite and anatase. Some researchers (Teufer and Temple, 1966) describe it as a pseudorutile phase ($Fe_2Ti_3O_9$), characterized by X-ray diffraction patterns intermediate between ilmenite and rutile. The color of leucoxene varies widely—from brown and reddish tones to yellow, gray, and white—depending largely on the degree of alteration and titanium enrichment, with lighter colors indicating lower iron content (Temple, 1966; Mohamed, 1987; Ibrahim, 1995; Elsner, 2010). The leucoxenization process also affects physical properties such as density and magnetic behavior, while increasing impurity levels of SiO_2 and Al_2O_3 (Frost *et al*., 1986; Hugo and Cornell, 1991). Morphologically, leucoxene commonly occurs as rounded, opaque grains with rough, pitted surfaces (Fig. 6.a,b), and its specific gravity ranges from 3.5 to 4 depending on the degree of iron removal. It is a common mineral in the studied sediments, with its vertical distribution presented in Table (5), showing decreasing average concentrations with depth, and its lateral variation illustrated in (Fig.7). In modern usage, leucoxene refers to a commercial titanium-rich concentrate (>70 wt.% TiO_2), consisting mainly of pseudorutile and rutile (Frost *et al*., 1983).

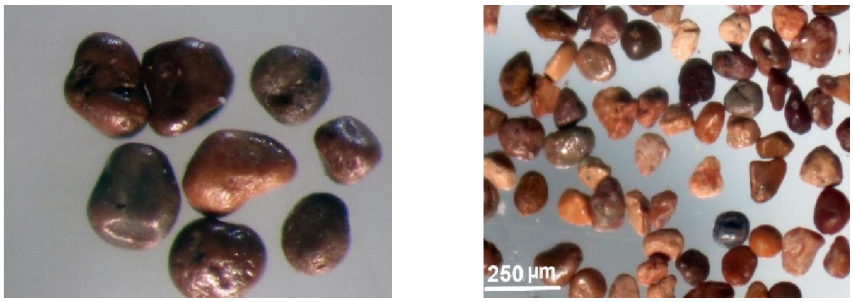

a) **b)**

Fig. 6: Photomicrographs show: a) dark brown rough pitted surface leucoxene b) brown, white, and black color remaining of ilmenite.

Table 5: The percentage of Leucoxene mineral

	Leucoxene		
S. No.	**First Meter**	**Second Meter**	**Third Meter**
1	0.702	0.702	0.349
2	0.919	0.464	0.359
3	0.864	0.734	0.32
4	0.734	0.613	0.265
5	0.627	0.431	0.291
6	0.646	0.543	0.128
7	0.655	0.365	0.345
8	0.572	0.422	0.19
9	0.673	0.441	0.319
10	0.643	0.35	0.208
11	0.77	0.298	0.221
12	0.486	0.237	0.102
13	0.488	0.491	0.326
14	0.431	0.376	0.208
15	0.46	0.286	0.237
16	0.513	0.498	0.366
17	0.528	0.492	0.186
18	0.632	0.385	0.291
19	0.51	0.427	0.304
20	0.563	0.528	0.361
Min.	0.431	0.237	0.102
Max.	0.919	0.734	0.366
Ave.	0.6208	0.45415	0.2688

S. No. = Sample Number Min.=Minimum Max. =Maximum Ave.=Average

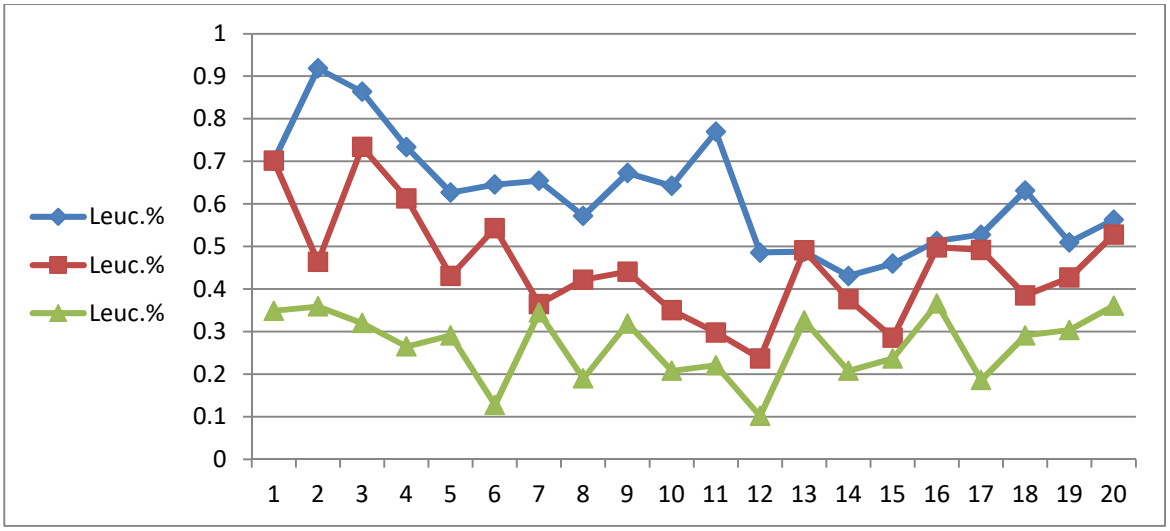

Fig. 7: Lateral distribution of leucoxene in the first, second, and third meters

The Non-opaque minerals

Rutile

Rutile is one of the three polymorphic forms of titanium dioxide (TiO_2), alongside anatase and brookite, and represents the most stable and common form in nature (Deer *et al*., 1975). Egyptian black sand rutile has been classified into several types based on composition and optical properties, including ilmenorutile, ferriferous rutile, secondary rutile, and translucent varieties (Hammoud, 1966). It occurs in two main genetic forms: The occurrence of rutile is attributed to two different origins. One variety crystallized directly from magma and is therefore considered primary rutile, whereas the other developed later through the transformation of Fe–Ti oxide minerals, especially ilmenite, and is referred to as secondary rutile (Dabbour, 1997).The color of primary rutile varies widely—from brown and red to yellow and green—due to the presence of impurity elements such as iron, niobium, and tantalum, whereas secondary rutile is typically black and opaque. Morphologically, most rutile grains are subrounded to well-rounded (~70 wt.%), with smaller proportions of tabular (~20 wt.%) and angular forms (~10 wt.%), while well-formed euhedral crystals are rare (Barakat, 2016). Under microscopic examination, rutile appears in various colors (reddish-brown, black, yellow) and shapes, including prismatic and rounded forms with occasional twinning (Fig. 8.a–d). Its magnetic susceptibility varies depending on iron content, allowing partial concentration in low magnetic fields. Rutile is widely distributed in the studied sediments and occurs in both magnetic and non-magnetic fractions, with its vertical distribution presented in Table (6), showing decreasing average concentrations with depth, and its lateral distribution illustrated in (Fig.9). ESEM analysis of selected grains is shown in (Fig. 8.e,f). Economically, Egyptian rutile and leucoxene are used in the manufacture of welding electrodes; however, local production is insufficient to meet demand, necessitating imports from countries such as India and Australia.

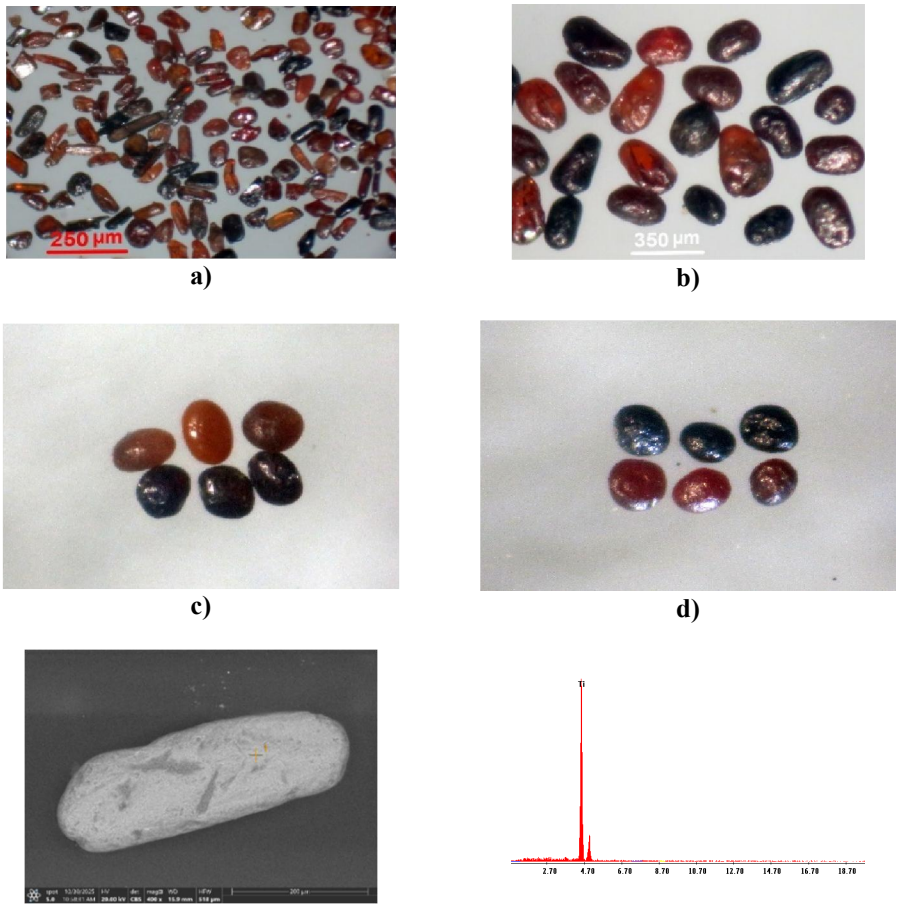

Fig. 8: Photomicrographs show: a) red to black, brown, and orange to yellowish prismatic rutile, b) rounded rutile, c) Red and black oval rutile, d) Red and black discoidal and rounded rutil, e,f) EDX and BSE image of rutile.

Table 6: The percentage of Rutile mineral

	Rutile		
S. No.	**First meter**	**Second meter**	**Third meter**
1	0.29	0.2	0.186
2	1.031	0.25	0.121
3	0.911	0.183	0.126
4	0.306	0.207	0.226
5	0.389	0.391	0.067
6	0.839	0.235	0.208
7	0.397	0.365	0.325
8	0.57	0.28	0.158
9	0.31	0.233	0.09
10	0.458	0.11	0.064
11	0.479	0.235	0.153
12	0.375	0.241	0.128
13	0.295	0.187	0.146
14	0.209	0.208	0.125
15	0.251	0.224	0.125
16	0.376	0.22	0.168
17	0.303	0.131	0.122
18	0.345	0.172	0.067
19	0.251	0.212	0.139
20	0.37	0.215	0.147
Min.	0.209	0.11	0.064
Max.	1.031	0.391	0.325
Ave.	0.43775	0.22495	0.14455

S. No. = Sample Number Min.=Minimum Max. =Maximum Ave.=Average

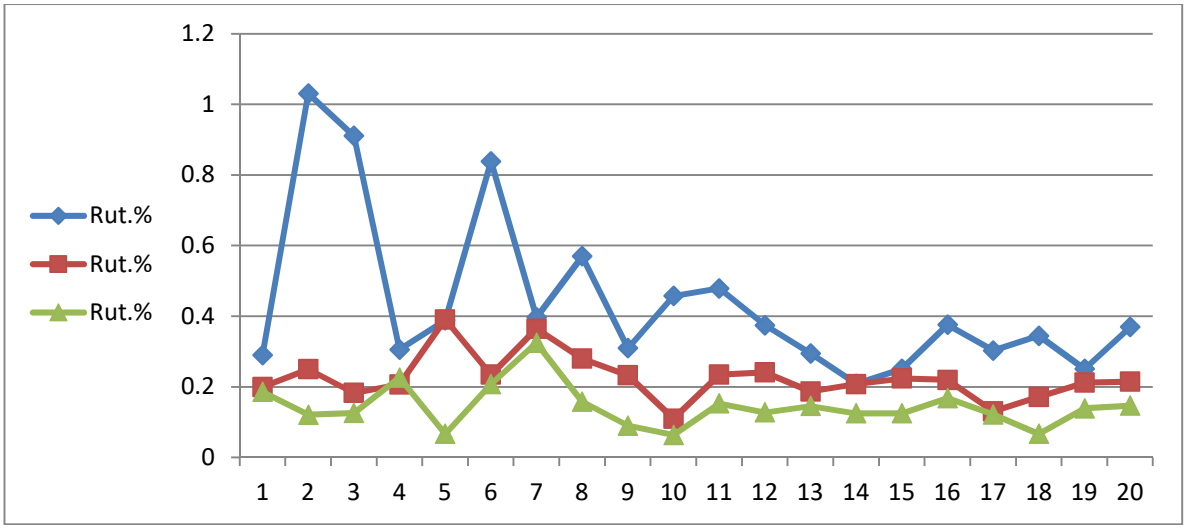

Fig. 9: Lateral distribution of rutile in the first, second, and third meters

Garnet

Garnet in Egyptian black sands is most commonly characterized by a pale pink color and exhibits moderate magnetic susceptibility that varies slightly with its chemical composition (Milner, 1962). Garnet minerals typically form within metamorphic and certain igneous rocks and are also present as detrital grains in placer deposits. Chemically, garnets follow the general formula $A_3B_2(SiO_4)_3$, where A-site cations include Mg^{2+}, Fe^{2+}, Mn^{2+}, and Ca^{2+}, and B-site cations include Cr^{3+}, Al^{3+}, and Fe^{3+}. They are classified into two main series: the pyralspite group (pyrope, almandine, and spessartine) and the grandite group (uvarovite, grossular, and andradite), with compositional variation occurring within each series but not between them (Deer *et al*., 1975). Garnet occurs in a wide range of colors except blue, including red, orange, violet, yellow, green, and colorless varieties, all of which are observed in Egyptian black sands (Rous, 1986). Due to its hardness, angular fracture, and resistance to physical and chemical weathering, garnet is highly valued in abrasive applications and has largely replaced quartz in sandblasting for both efficiency and environmental reasons (Kendall, 1997). According to El-Kammar *et al*. (2010), Egyptian garnet is predominantly composed of almandine (~70.9 wt.%), followed by spessartine, pyrope, and minor grossular. Mineralogical studies (Dewedar, 1998) indicate that garnet grains are generally coarser than associated heavy minerals and may show etching features inherited from source rocks. Magnetic separation studies (El-Nahas, 2002) revealed that most garnet grains concentrate at 0.20 ampere, with decreasing recovery at higher currents. In the study area, garnet occurs mainly as angular to subrounded grains with hardness around 7 (Mohs scale) and moderate magnetic behavior, displaying colors from rose to red with occasional inclusions (Fig. 10.a). It is a common accessory mineral in all studied sediments, with its vertical distribution presented in Table (7), showing decreasing average concentrations with depth, and its lateral distribution illustrated in (Fig. 11). ESEM analysis (Fig. 10.b–d) indicates that most analyzed grains are dominated by almandine composition ($Fe_3Al_2Si_3O_{12}$), often containing inclusions of ilmenite.

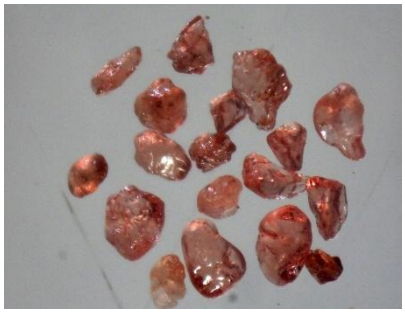

a)

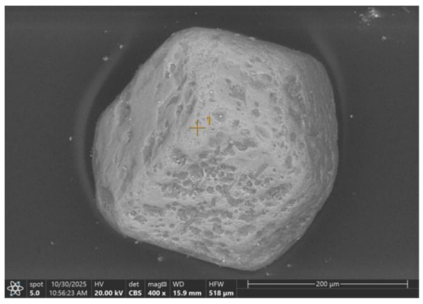

b)

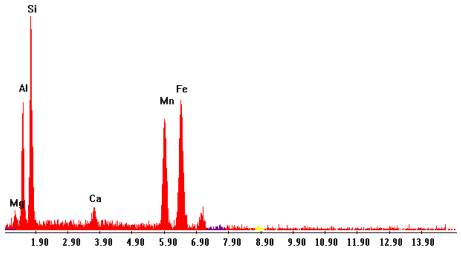

c)

Element	Weight %
O	8.8
Mg	2.8
Al	15.0
Si	27.8
Ca	3.6
Mn	2.3
Fe	39.7
Total	100

d)

Fig. 10: Photomicrographs show: a) Rose to red garnet, b,c) EDX and BSE image of almandine garnet, d) chemical compositions of garnet.

Table 7: The percentage of Garnet mineral

	Garnet		
S. No.	**First Meter**	**Second Meter**	**Third Meter**
1	1.845	1.275	1.2
2	1.919	1.122	0.975
3	2.191	1.993	0.795
4	1.325	1.31	1.077
5	1.832	1.659	0.786
6	2.363	1.011	0.854
7	1.868	1.077	0.806
8	1.300	1.138	0.559
9	1.759	0.98	0.87
10	1.412	0.556	0.616
11	2.234	0.855	0.8
12	1.201	0.895	0.712
13	1.202	1.1300	0.672
14	1.348	0.859	0.58
15	0.891	0.705	0.895
16	1.179	0.55	0.725
17	1.768	1.312	0.979
18	2.522	0.791	0.986
19	2.082	0.667	0.639
20	1.6900	1.441	1.216
Min.	0.891	0.55	0.559
Max.	2.522	1.993	1.216
Ave.	1.69655	1.0663	0.8371

S. No. = Sample Number Min.=Minimum Max. =Maximum Ave.=Average

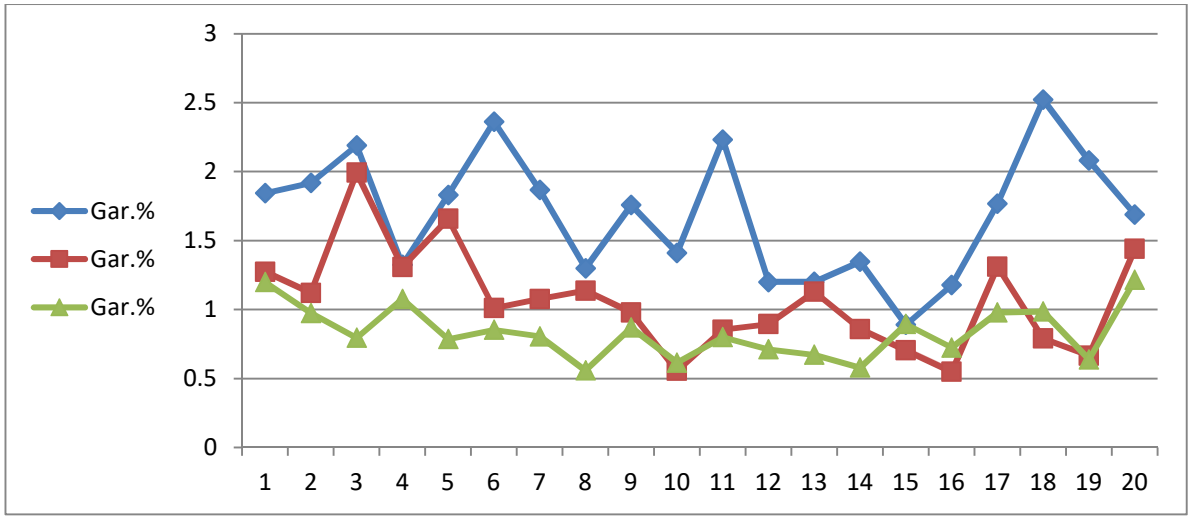

Fig. 11: Lateral distribution of garnet in the first, second, and third meters

Zircon

Zircon is a non-magnetic and non-conductive heavy mineral that can be effectively separated from other minerals based on differences in specific gravity, magnetic susceptibility, and electrical conductivity (Barakat, 2004). However, the presence of inclusions—some of which may be magnetic or conductive—can influence its separation behavior. Egyptian black sand zircon exhibits variable magnetic properties due to such inclusions, and has been classified into strongly magnetic (1 wt.%), moderately magnetic (8 wt.%), and predominantly non-magnetic types (91 wt.%) (Rittman and Nakhla, 1958). Mineralogically, zircon is primarily zirconium silicate with minor amounts of uranium, thorium, titanium, and rare earth elements. It occurs mainly as colorless, transparent grains with low radioactive content (~82.28 wt.%), alongside a smaller proportion of darker, radioactive varieties (~17.72 wt.%) (Dabbour, 1994). Additional classifications based on color include clear, smoky, dusky, and other colored varieties (Zaghloul and Kamel, 1966), while compositional categories range from clear to metamict zircon depending on trace element content (Rozendaal & Philander, 2000).

Zircon grains commonly exhibit prismatic bipyramidal forms with varying degrees of roundness and are often characterized by inclusions such as magnetite, ilmenite, hematite, and occasionally radioactive minerals like monazite and xenotime (Hammoud, 1973; Dabbour, 1973). These inclusions influence grain color—ranging from colorless and pale pink to reddish-yellow—and may weaken grain stability (Carrol, 1953; Hassan, 2005). Morphologically, zircon occurs as euhedral to sub-rounded grains (Fig. 12.a–d), and is distributed in both magnetic and non-magnetic fractions, particularly at 1.5A separation. ESEM analyses of selected grains are presented in (Fig. 12.e–g). Quantitative data (Table 8) indicate that zircon content decreases with depth across the studied profiles, while its lateral distribution is shown in (Fig. 13). Economically, zircon is a valuable mineral widely used in refractory materials, especially in glass and aluminum industries due to its resistance to high temperatures and corrosion (Sinha, 1982), as well as in ceramics as an opacifier owing to its high reflectivity and thermal stability.

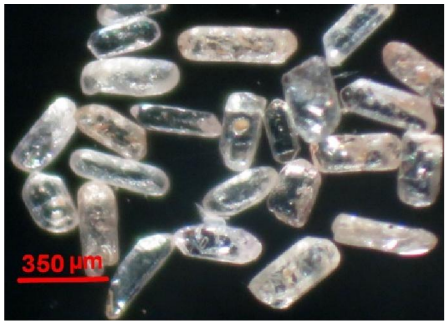

a)

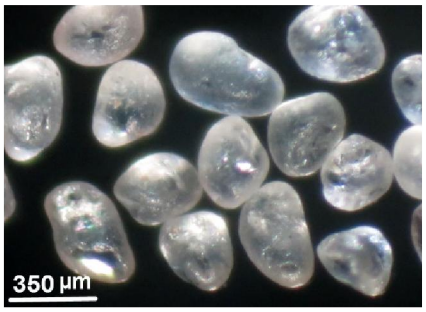

b)

c)

d)

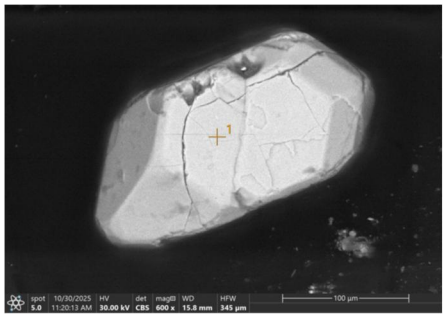

e)

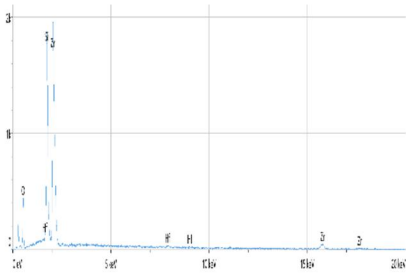

f)

Element	Wt. %
O	38.0
Si	27.6
Zr	32.7
Hf	1.7
Total	100

g)

Fig. 12: Photomicrographs show: a) colorless prismatic zircon, b) colorless rounded zircon, c) reddish yellow prismatic with rounded termination zircon, d) honey color zircon, e&f)) EDX and BSE image of zircon, g) chemical compositions.

Table 8: The percentage of Zircon mineral

	Zircon		
S. No.	**First Meter**	**Second Meter**	**Third Meter**
1	0.904	0.583	0.677
2	0.083	0.519	0.338
3	0.050	0.584	0.437
4	0.673	0.638	0.355
5	0.826	0.156	0.322
6	0.383	0.280	0.447
7	0.693	0.355	0.389
8	0.124	0.661	0.314
9	0.713	0.574	0.109
10	1.117	0.243	0.207

11	1.337	0.470	0.188
12	0.849	0.568	0.279
13	0.903	0.404	0.344
14	0.462	0.676	0.311
15	0.569	0.547	0.306
16	0.543	0.450	0.325
17	0.863	0.561	0.256
18	0.930	0.392	0.322
19	0.598	0.491	0.299
20	0.903	0.501	0.421
Min.	0.05	0.156	0.109
Max.	1.337	0.676	0.677
Ave.	0.67615	0.48265	0.3323

S. No. = Sample Number Min.=Minimum Max. =Maximum Ave.=Average

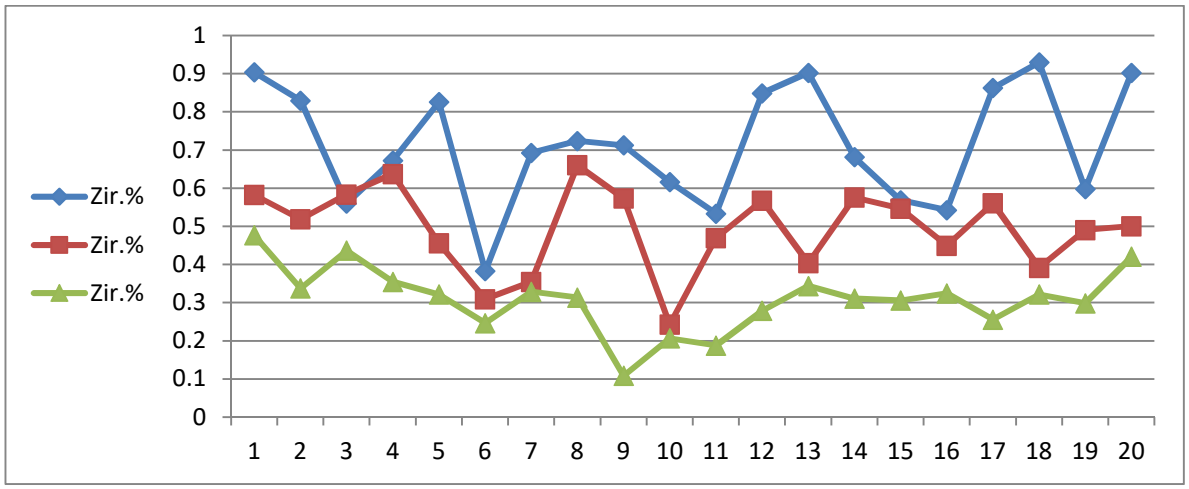

Fig. 13: Lateral distribution of zircon in the first, second, and third meters.

Monazite

As a major carrier of rare earth elements, monazite consists mainly of phosphate compounds enriched in cerium, lanthanum, praseodymium, and neodymium. These elements represent the overwhelming majority of its rare earth composition, reaching approximately 92 wt.% of the total REE content. Minor substitutions may include yttrium and trace elements such as Ca, Mg, Mn, Fe, Al, Zr, Be, and Sn. Structurally, monazite forms solid-solution series with related minerals such as huttonite and brabantite through coupled substitutions (Harlov *et al*., 2007). It is weakly magnetic (Milner, 1962) and can be classified into several compositional types, including (Ce)-, (La)-, (Nd)-, and (Sm)-monazite, based on dominant rare earth elements (Van Emden *et al*., 1997). Studies indicate that Egyptian black sand monazite occurs in relatively low concentrations, ranging from trace amounts up to 0.5 wt.% in highly enriched zones, with Ce_2O_3 being the dominant. Chemical analyses reveal significant contents of ThO_2 and U_3O_8, confirming its importance as a source of rare earth elements and radioactive materials (Hilal and El-Gohary, 1959; Dabbour, 1994).

Mineralogically, monazite occurs as well-rounded, high-sphericity grains, typically free of inclusions, and exhibits a wide range of colors including colorless, yellow, brown, red, and black (Fig. 14.a,b), with lemon-yellow and honey-yellow being the most common (Zaghloul and Kamel, 1965). It is found as an accessory mineral in fine-grained sediments and can be separated at magnetic field strengths of 0.5–1.0 A. Quantitative distribution data (Table 9) show decreasing concentrations with depth, while lateral variations are illustrated in (Fig. 15). ESEM analyses of selected grains are presented in (Fig. 14.c–e), indicating that the studied samples are predominantly of the (Ce)-monazite type. Economically, monazite is a major source of rare earth elements and is utilized in various industrial applications, including catalysis, electronics, alloys, ceramics, and nuclear energy due to its thorium content (Tourre, 1999).

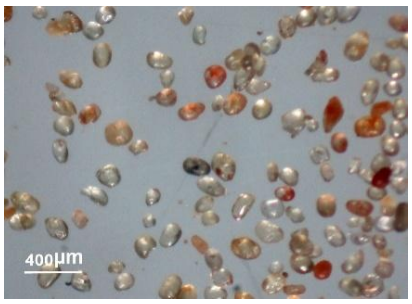

a)

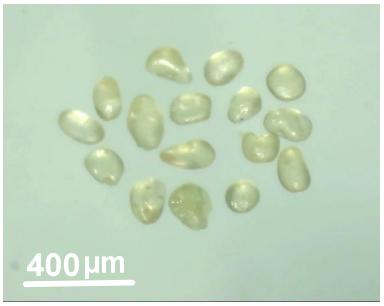

b)

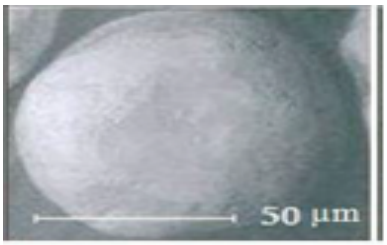

c)

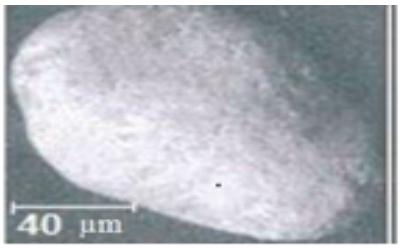

d)

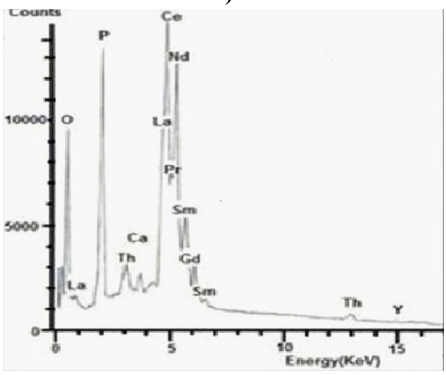

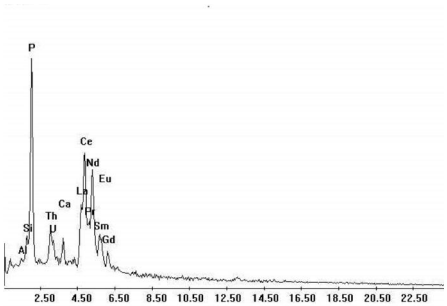

Element	Wt.%	Wt. %)	Element	Wt.%	Wt. %)
P2O5	29.04	27.66	ThO2	2.4	6.12
Ce2O3	19.55	29.77	U3O8	1.1	1.16
La2O3	9.41	14.23	SiO2	0.99	0.68
Nd2O3	12.22	11.54	CaO	0.7	0.8
Sm2O3	3.5	2.82	Fe2O3	0.4	0.2
Gd2O3	3.3	1.92	MgO	0	0.1
Eu2O3	1.42	0.24	Al2O3	0.37	0.17
Y2O3	0.91	0.17	PbO2	0.19	0.21
Pm2O3	6.71	0.7	Sc2O3	0.11	0.13
Tm2O3	2.71	0.25	Pr2O3	0.32	0.37
Yb2O3	3.7	0.63	At2O	0.7	0.11
Dy2O3	0.25	0.02	----------	----------	----------
Total	-------- --	----------	----------	100	100

e)

Fig. 14: Photomicrographs show: a) colorless rounded monazite, b) lemon yellow monazite, c&d) EDX and BSE image of monazite, e) chemical compositions of monazite.

Table 9: The percentage of monazite mineral

	Monazite		
S. No.	**First Meter**	**Second Meter**	**Third Meter**
1	0.098	0.026	0.043
2	0.083	0.033	0.000
3	0.787	0.085	0.002
4	0.075	0.029	0.025
5	0.005	0.007	0.014
6	0.021	0.002	0.001
7	0.031	0.025	0.005

8	0.032	0.048	0.033
9	0.028	0.050	0.000
10	0.002	0.003	0.037
11	0.009	0.032	0.002
12	0.001	0.005	0.006
13	0.045	0.003	0.004
14	0.001	0.036	0.017
15	0.045	0.016	0.000
16	0.013	0.000	0.000
17	0.004	0.049	0.000
18	0.034	0.000	0.014
19	0.001	0.013	0.029
20	0.001	0.039	0.009
Min.	0.001	0	0
Max.	0.787	0.085	0.043
Ave.	0.0658	0.02505	0.01205

S. No. = Sample Number Min.=Minimum Max. =Maximum Ave.=Average

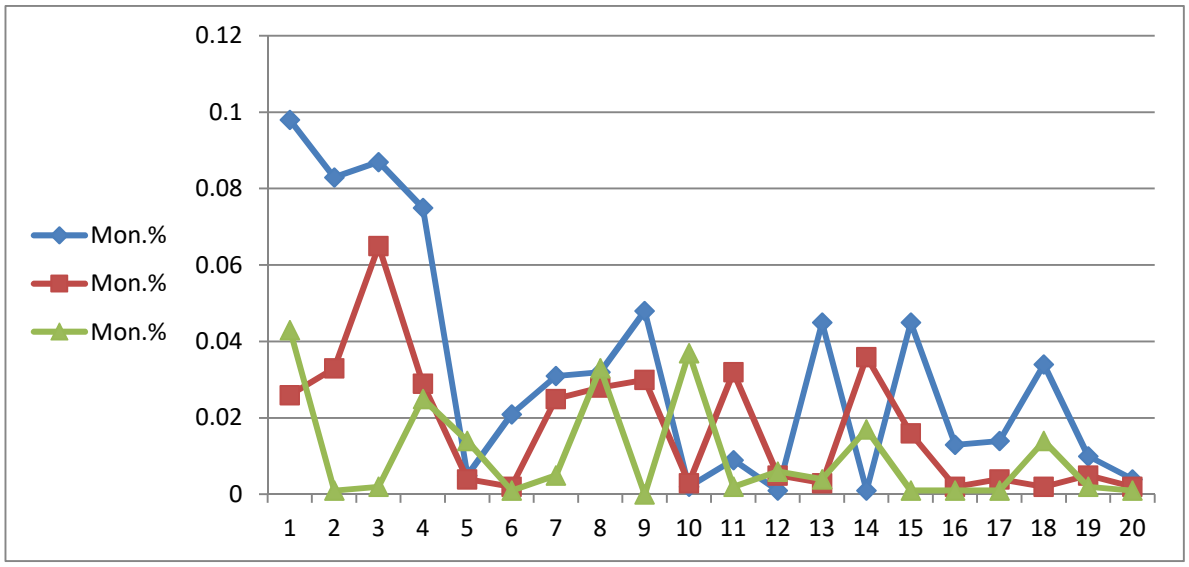

Fig. 15: Lateral distribution of monazite in the first, second, and third meters.

Non-Economic Minerals

Green Silicates

Green silicate minerals are commonly present in the studied sediments and are typically separated using heavy liquid techniques such as bromoform (specific gravity 2.86 g/cm³). These minerals are mainly concentrated in the second magnetic fraction (0.5 A), with smaller amounts occurring at 1.0 A and decreasing with increasing magnetic field strength. This group includes a wide range of silicate minerals with different structural types, such as sheet silicates (mica group, including muscovite and biotite), single-chain silicates (pyroxenes such as bronzite, hypersthene, diopside, hedenbergite, augite, aegirine, and jadeite), and double-chain silicates (amphiboles including anthophyllite, tremolite, actinolite, hornblende, and others), many of which are altered into chlorite, serpentine, or carbonate minerals. It also comprises isolated tetrahedral silicates such as garnet and olivine, along with less common minerals like kyanite, sillimanite, andalusite, staurolite, and epidote group minerals.

Biotite, a member of the dark mica group with the general formula $K(Mg, Fe)_3(AlSi_3O_{10})(F,OH)_2$, represents a solid-solution series between iron-rich annite and magnesium-rich phlogopite, and is often referred to as “black mica” in contrast to muscovite (“white mica”) (Fig. 16.a,b). It typically occurs as tabular to prismatic crystals with well-developed basal cleavage, forming flexible sheets due to weak bonding between layers. Biotite displays a wide range of colors from dark brown and greenish-brown to black, and may appear yellow or whitish when weathered, with a vitreous to pearly luster and varying transparency. It is widely distributed in the studied sediments, particularly within the 0.5 A magnetic

fraction. Quantitative analysis (Table 10) shows that green silicate minerals decrease in concentration with depth, while their lateral distribution is illustrated in (Fig. 17).

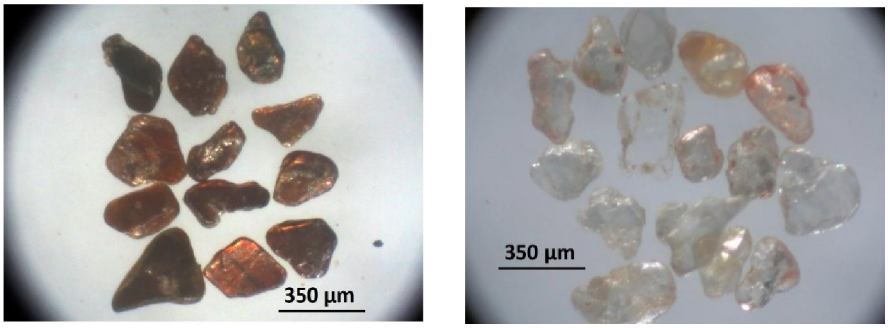

Fig. (16): a) Photomicrographs of vitreous to pearly luster biotite. b) Photomicrographs of muscovite.

Table 10: The percentage of green silicate mineral

	Green silicate		
S. No.	**First Meter**	**Second Meter**	**Third Meter**
1	13.706	12.809	10.195
2	23.245	14.682	12.267
3	20.52	16.31	12.342
4	16.875	14.476	10.876
5	19.604	13.06	11.473
6	20.624	15.513	14.553
7	22.754	13.779	14.02
8	17.639	15.001	12.582
9	21.369	13.964	10.032
10	33.055	15.588	13.492
11	23.619	16.257	11.689
12	25.302	16.778	11.824
13	23.797	15.489	11.728
14	22.689	14.643	11.777
15	19.221	14.455	13.288
16	18.853	15.408	12.966
17	20.995	14.693	12.016
18	24.176	16.259	7.934
19	28.98	17.05	10.962
20	29.03	17.987	15.3
Min.	13.706	12.809	7.934
Max.	33.055	17.987	15.3
Ave.	22.30265	15.21005	12.0658

S. No. = Sample Number Min.=Minimum Max. =Maximum Ave.=Average

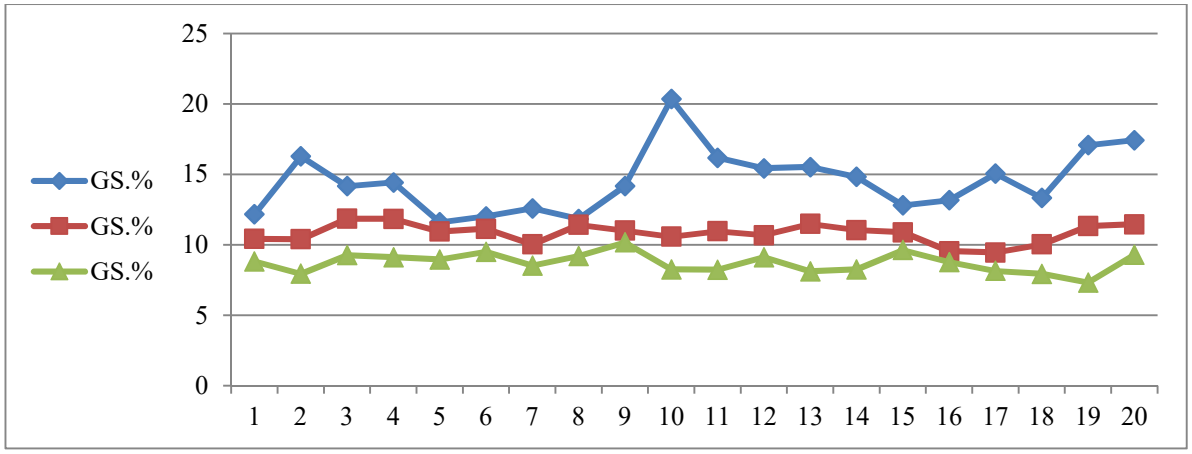

Fig. 17: Lateral distribution of Green Silicate in the first, second, and third meters.

Accessory minerals

Hematite Fe_2O_3

Hematite is the primary iron ore, mainly formed through the alteration of magnetite and other iron-bearing minerals, particularly pyrite, often resulting in pseudomorphic forms such as goethite. Non-crystalline hematite may also originate from the transformation of limonite. It typically appears as reddish-brown to black grains with elongated, rod-like, angular to sub-angular shapes and exhibits either metallic or earthy luster (Fig. 18.a). The chemical composition of hematite grains was analyzed using Environmental Scanning Electron Microscopy (ESEM), as illustrated in (Fig. 18.b).

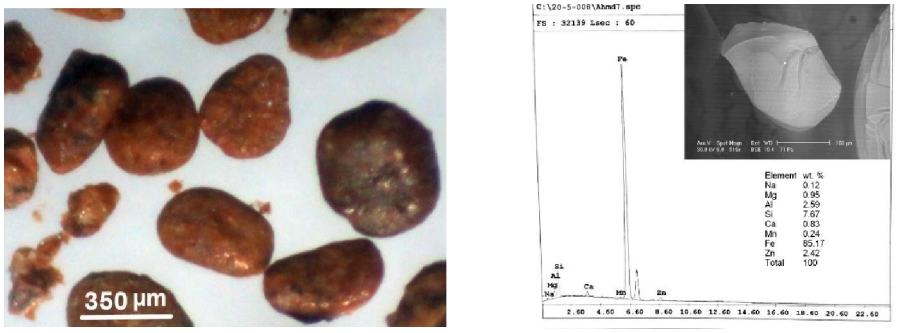

a) b)

Fig. 18: Photomicrographs show: a) granular, angular to sub-angular hematite and b) EDX and BSE image of hematite grains

Staurolite $Fe^{2+}_2\ Al_9\ O_6\ (SiO_4)_4(O, OH)_2$

Staurolite grains $(Fe, Mg)_2\ (Al, Fe)_9\ O_6\ (SiO_4)(OOH)$ were separated at magnetic field strength 0.2A and 0.5A and were picked using binocular stereomicroscope. Barakat (2016) stated that: Staurolite represent about 3% of garnet concentrate and it has been used as an abrasive. Staurolite occur as yellow road like (Fig.19.a). Picked staurolite grain were investigated using ESEM and their chemical compositions are shown in (fig.19.b).

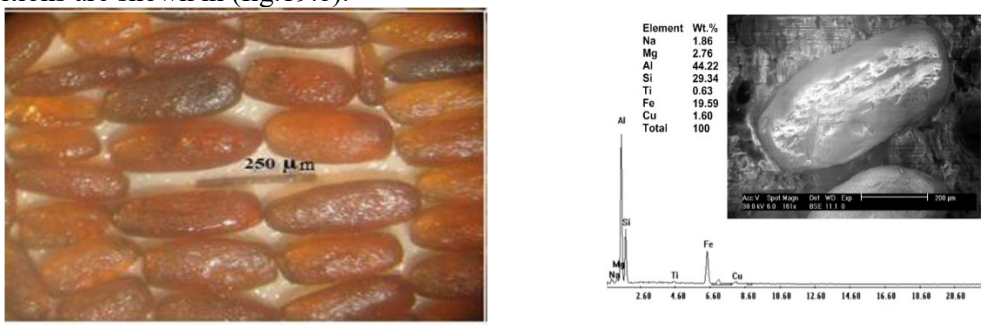

Fig. 19 show: a) Photomicrographs Yellow staurolite grains. b) EDX and BSE image of staurolite.

Titanite (Sphene) Ca Ti SiO_5

Titanite occurs as a widespread accessory mineral in the investigated sediments. Its grains are commonly yellow to brownish-yellow in color and exhibit a distinctive vitreous sheen (Fig. 20a). Most titanite grains are subhedral to anhedral and possess imperfect cleavage. During magnetic separation, the mineral was mainly recovered from the 1.0 A magnetic fraction, with only minor occurrences in the 0.5 A fraction. Selected grains were subjected to ESEM–EDX analysis to determine their chemical characteristics, and the analytical results are illustrated in Figure (20b).

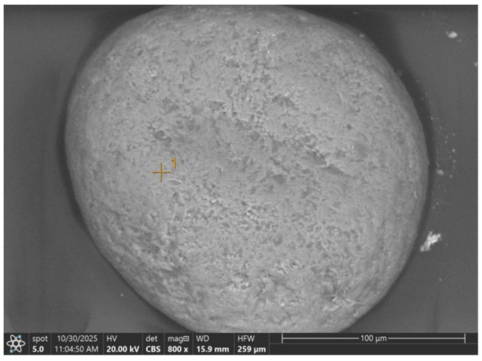

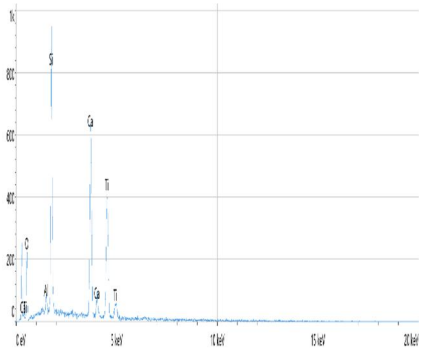

Element	Weight %
O	26.4
Al	1.0
Si	20.1
Ca	24.2
Ti	28.2

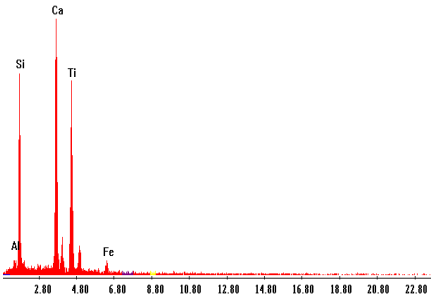

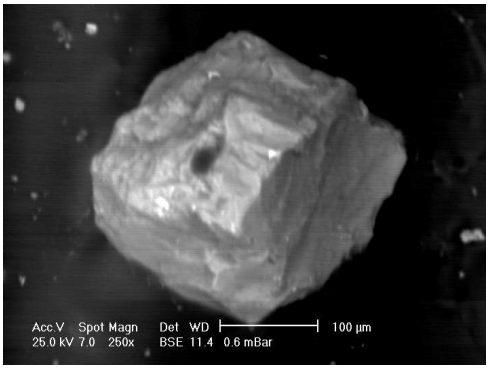

Element	Wt.%
Al	1.86
Si	25.16
Ca	33.03
Ti	36.85
Fe	3.18
Total	100

Fig. (20. a) Photomicrographs yellowish to brownish yellow titanite b) EDX and BSE image of titanite.

Apatite $Ca_5 (PO_4)_3F$

As the most common phosphate mineral, apatite plays an important role as a natural reservoir of phosphorus required for biological processes and plant nutrition. It is also a fundamental component of

bones and teeth in both humans and animals. Within the investigated samples, apatite was identified as brown-colored grains with wedge-shaped and irregular morphologies (Fig. 3.23a). Detailed mineralogical characterization was carried out using ESEM–EDX analyses, and the resulting micrographs and chemical data are illustrated in Figures (3.23b–f).

a)

Element	Weight % S1	Weight % S2
Al	1.7	00
Si	2.7	00
P	21.0	25
Ca	65.4	75
Fe	3.1	00
Zn	1.8	00
Cu	2.1	00
Si	2.2	00
Total	100	100

b)

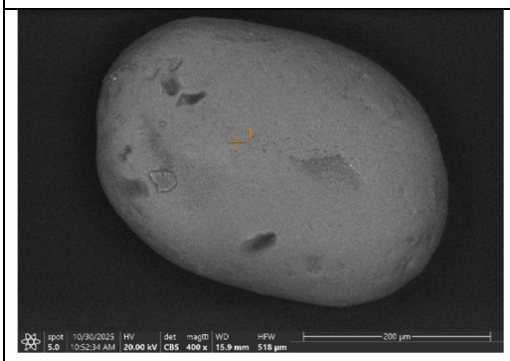

c) S1

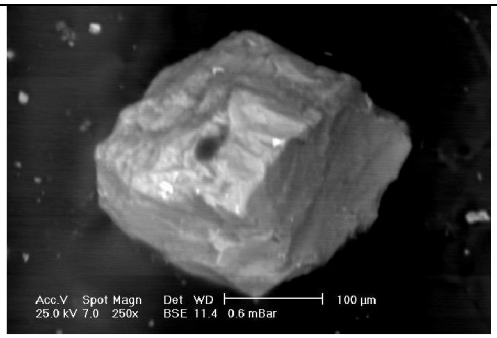

d) S2

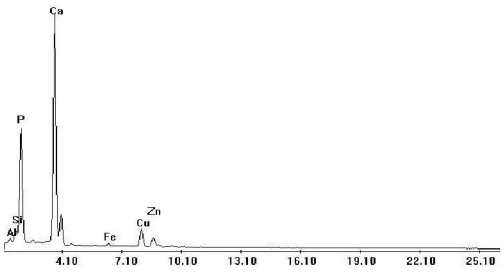

e) S1

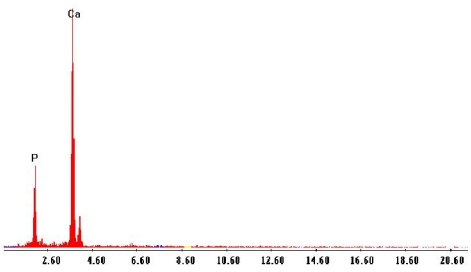

f) S2

Fig. 21: a) Photomicrographs apatite**. b)** EDX and BSE image of apatite.

Conclusion

The distribution and concentration of heavy minerals within the Baltim–El Burullus coastal sediments are mainly controlled by marine processes, especially wave action and the dominant eastward longshore current along the Mediterranean coast. These processes play an important role in sorting and concentrating heavy minerals into alternating dark and light layers, which represent one of the characteristic features of beach deposits in the study area (Soliman, 1964).

The thickness and continuity of these heavy mineral accumulations are affected by seasonal changes in wind directions, particularly the northwestern, northeastern, southwestern, western, and northern winds, which continuously influence sediment movement and redistribution along the coast (Misak &

Attia, 1983). As a result, heavy mineral concentrations may occur either as visible streaks on the surfaces of coastal dunes or as buried layers within subsurface sediments.

The studied sediments contain several economically valuable heavy minerals. Ilmenite is the most abundant mineral, with concentrations ranging from 1.701% to 16.791% and an average of 6.033%. Magnetite ranges between 0.015% and 1.165% with an average of 0.19%, while garnet concentrations vary from 0.55% to 2.522% with an average value of 1.20%. Zircon contents range from 0.05% to 1.337% with an average of 0.497%, whereas rutile concentrations vary between 0.064% and 1.031% with an average of 0.269%. Leucoxene ranges from 0.102% to 0.919% with an average of 0.448%, while monazite occurs in relatively low concentrations ranging from 0% to 0.787% with an average of 0.034%. Apatite, titanite, and staurolite are present only in trace amounts.

The results also show that heavy mineral concentrations generally decrease with increasing depth, which reflects the influence of depositional conditions and hydrodynamic sorting processes on the vertical distribution of black sand minerals. Overall, the Baltim–El Burullus coastal zone can be considered a promising area for economically important heavy mineral deposits and provides valuable information about the sedimentological and mineralogical characteristics of the northern Nile Delta coastal environment.

Reference

Anwar, Y. M. and A. M. El Bouseily, 1972. Subsurface studies of the black sand deposits at Rosetta, Nile mouth Egypt. Part II, mineralogical studies. Bull. Fac. Sci., Alexandria Univ., Egypt, (10)141-150.

Arafa, E. H. M., 1990: mineralogical and sedimentalogical studies of some sediments from Egypt and Sudan. Ph. D. thesis, Fac. of Sci. Cairo Nuiv., Egypt.

Bai, J., B. Cui, B. Chen, K.Zhang , W.Deng , H. Gao & R. Xiao, 2011. Spatial distribution and ecological risk assessment of heavy metals in surface sediments from a typical plateau lake wetland, China. Ecological Modelling, 222(2), 301-306. doi: 10. 1016/j. ecolmodel. 2009. 12.002

Barakat, M.G. 2004: Sedimentological studies and evaluation of some black sands deposits on the northern coast of Egypt. M.Sc. Thesis, Fac.Sci. Alexandria University, Egypt, 176 p.

Barakat, M.G. 2016: Evaluation and mineralogy of beach economic minerals especially ilmenite for the top meter in the Egyptian black sand, east Rosetta, Egypt. Ph. D. Thesis, Fac. Sci. Zagazig university, Egypt, 284p.

Basta, E. Z. 1972: different types of ilmenite-magnetite intergrowth and their origin. Bull., Fac. Sci., Univ.,(44) 195-212.

Boctor, N. Z. 1966. Ore microscopic studies of the opaque minerals in Rosetta-Damietta black sands. Unpub. M.Sc. Thesis, Fac. Sci., Cairo Univ., Cairo, Egypt.

Bramha, S. N., A. K. Mohanty, K. K. Satpathy, K. V. Kanagasabapathy, S. Panigrahi, M. K. Samantara, & M. V. R. Prasad, 2014. Heavy metal content in the beach sediment with respect to contamination levels and sediment quality guidelines: a study at Kalpakkam coast, southeast coast of India. Environmental earth sciences, 72(11), 4463-4472. doi:10.1007/s12665-014-3346-y

Bryan, K.R., A. Robinson, and R.M. Briggs, 2007. Spatial and temporal variability of titanomagnetite placer deposits on a predominantly black sand beach. Marine Geology, (236) 45-59.

Carroll, D., 1953: Weatherability of zircon. J. Sed. Pet., Vol. 23, 116p.

Chaudhuri, J.N.B. and H. Newesely, 1990: Transformation of ilmenite FeTiO3 to leucoxene TiO2 under the influence of weathering reactions. Indian Journal of Technology, (28) 13- 23.

Dabbour, G. A. 1973. Physical properties and distribution of zircon in some Egyptian deposits. Unpub. M.Sc. Thesis, Fac. Sci. Cairo Univ., Cairo, Egypt.

Dabbour, G. A. 1994. The Egyptian placer deposits-a potential source for Nuclear Raw Materials, Second Arab Conference on the peaceful uses of Atomic Energy, Cairo, 5-9 Nov. part 11: A, Scientific Paper.

Dabbour, G.A. 1995: Nuclear and valuable materials in the Egyptian black sands. Proc. Inter. Conf. Energy for Continuous Development Challenge in Developing Countries, Arab Min. Petro. Assoc., Cairo.

Dabbour, G. A. 1997. Mineralogical study on the opaque minerals and secondary rutile from the Egyptian black sand. Proceding of the Egyptian Academy of Science. V. 47.

Deer, W.A., R.A. Howie, and J. Zussman, 1975: An introduction to the rock forming minerals. Longman group Ltd., London, 528p.

Dewedar, A. A. M. 1998: Comparative studies on the heavy minerals in some black sands from Sinai and east Rosetta, with contribution to the mineralogy and economics of their garnets. Unpubl. Ph.D. Thesis, Fac. Sci., El Menoufia Univ., Shibin El-kom, Egypt.

Eisenmann, M.D. 2001: Elutriation technology in heavy mineral separations. M.Sc. Thesis, Faculty of Virginia polytechnic Institute and state University.

El Balaksy, S. S. 2003: Minerological studies for the economic minerals in the sand dune belts at Baltim area. Unpub. Ph D. Thesis. Fac. Sci. Ain Shams Univ., Cairo, Egypt.

El Baz, S.M., & M.M. Khalil, 2018: Assessment of trace metals contamination in the coastal sediments of the Egyptian Mediterranean coast. Journal of African Earth Sciences 143, 195-200. doi: 10.1016/j.jafrearsci.2018.03.029

El Gohary, R., M. Bahadir, & M. Elbisy, 2017: Risk assessment of heavy metals in new Damietta harbor along the Egyptian Mediterranean coast. Int. J. Multidiscip. Curr. Res. 5, 598-612

El-Kammar, A. A., A. A., Ragab and M. I. Moustafa, 2010: Geochemistry of Economic Heavy Minerals from Rosetta Black Sand of Egypt. Journal of KAAL: Earth Science, Kingdom of Saudi Arabia, (22) No. 2, 1-25.

El-Nahas, H.A. 2002: Mineralogy, Evaluation and Upgrading Studies on Some Economic Minerals in Beach Black Sands. El Arish Area, Egypt. M.Sc. Thesis. Fac. Sci., El Minufiya University, Egypt, 162 p.

Elsner. H., 2010: Heavy minerals of economic importance. Assessment manual, Faculty of Geosciences of the University of Hannover: 218p., 31 Fig. 125 Tab. Flinter, B. H., (1955): A magnetic separation of some alluvial minerals in Malaya, Amer. Miner.,(44) No. 7-8, 751p.

El-Zeiny, A. 2010: Monitoring and Evaluation of some Pollutants at New Damietta – Damietta – Egypt (M.Sc. thesis). Damietta, Fac. of Sci. Mans. Univ.

Folk, R. L., 1980: Petrology of sedimentary rocks. Univ. Texas, Hemphill, Pup. Co., Austin, Texas, USA.

Force, E.R. 1991: Geology of titanium mineral deposits. Geol. Soc. Am., (259) 78.

Forstner, U., & G.T.W. Wittmann, 1983: Metal Pollution in Aquatic Environment, 2nd ed. Springer-Verlag, Berlin, Heidelberg, New York, 481 p.

Frost, M.T., I.E. Grey, I.R. Harrowfield, & K. Mason, 1983. The dependence of alumina and silica contents on the extent of alteration of weathered ilmenites from Western Australia.

Frost, M.T., I.E. Grey, I.R. Harrowfield, and Li, C. 1986: Alteration profiles and impurity element distributions in magnetic fractions of weathered ilmenite. Am. Mineral.,(71) 167-175.

Galanopoulou, S., A. Vgenopoulos, & N. Conispoliatis, 2009. Anthropogenic heavy metal pollution in the surficial sediments of the Keratsini harbor, saronikos Gulf, Greece. Water Air Soil Pollut. 202 (4),121-130.

Hammoud, N. S. 1966. Concentration of monazite from Egyptian black sand, employing industrial techniques, Unpub. M. Sc. Thesis, Fac. Sci., Cairo Univ.

Hammoud, N. S. 1973. Phisical and chemical properties of some Egyptian beach economic minerals in relation to their concentration problems. Unpub. Ph. D. Thesis, Fac. Sc. Cairo Univ., Cairo, Egypt.

Hammoud, N. S. 1975. A process of recovery low-chrmium high ilmenite from north Egyptian beach deposits. Proceeding of 11th International Mineral Processing Congress, Regione Autnoma Dell Sardengna, Italy.

Harlov, D.E., R. Wirth, and C.J. Hetherington, 2007: Replacement of monazite by a huttonite component: nature and experiment. Am. Min., 92: 1652-1664.

Harris, R.R., & M. C. F. Santos, 2000: Heavy metal contamination and physiological variability in the Brazilian mangrove crabs Ucides cordatus and Callinectes danae (Crustacea: Decapoda). Mar. Biol. (137), 691-703.

Hassaan, A. H. A., 2005: Evaluation of the heavy minerals in the coastal sand dunes, East Sabkhit Al-Tinna, North Sinai, Egypt. Ph. D. thesis, Fac., of Sci., Ain Shams Univ.

Hilal, O. and F. El-Gohary, 1959: Investigation of Egyptian Radioactive minerals, part I Monazite. Egypt. J. chem.., (2), No. 1,151-155.

Hogstand,C., & C. Haux, 2011: Binding and detoxification of heavy metals in lower vertebrates with reference to metallothionein. Comp Biochem Physiol C. (100), 137–214.

Hugo, V.E. and D.H. Cornell, 1991: Altered ilmenites in Holocene dunes from Zululand, South Africa: petrographic evidence for multistage alteration. S. Afr. J. Geol., (94) 365-378.

Hume, W. E. 1925: Geology of Egypt, Vol. 1, The surface features of Egypt, their determining causes and relation to geological structure. Egypt. Geol. Surv., 408 pp

Hussiny, N.A.; T.A. Lasheen, and M.E. Shalabi, 2008: Kinetic reduction of Rosetta ilmenite with coke Breeze and Beneficiation of the product. The Journal of ore dressing, (10), Issue20, 16-23.

Ibrahim, M. I. M. 1995: Investigation of physical properties of zircon and rutile to prepare high purity mineral concentrates from black sand deposits. Unpub. M.Sc. Thesis, Mansoura Univ., Mansoura, Egypt.

Jain, C. K., H. Gupta, & G. J. Chakrapani, 2008: Enrichment and fractionation of heavy metals in bed sediments of River Narmada, India. Environmental monitoring and assessment, 141(1), 35-47.

Kamel, O. A., A. H., Rasmy, A. Khalil, and R. Bakir, 1973: Mineralogical analysis and evaluation of black sands at eastern part of east side Nile section, Abu Khashaba area, Rosetta, Egypt. Ann. Geol. Surv. Egypt. (3) 227-247.

Kendall, T. 1997: Garnet nice work if you can get it. Industrial Minerals Magazine, March, p.31-41.

Kim, E.S., S.R. Cho, J.K. Park, T. Rack, & J.M. Lee, 2011: Distribution of heavy metals in the environmental samples of the saemangeum coastal area, Korea. In: Ishimatsu, A., Lie, H. J. (Eds.), Coastal Environmental and Ecosystem Issues of the East China Sea, 71-90.

Mallick, D., I.M. Shafiqul, A. Talukder, S. Mandol, M. Al Imran, & S. Biswas, 2016: Seasonal variability in water chemistry and sediment characteristics of intertidal zone at Karnafully estuary, Bangladesh. Pollution 2 (4), 411-423.

Mansour, S. M. M., 2009: Geology, Mineralogy and Radioactivity studies on Nuweibi area, Central Eastern Desert, Egypt. M. Sc. thesis, Fac., of Sci., Benha University.

Mc-Lemore, V.T. 2010: Distribution, origin and mineral resource potential of late cretaceous heavy mineral, Beach placer sand stone deposits, San Juan Basin, New Mexico. New Mexico Geological society Guidebook, 61st Field conference, four corners country, 197-212.

Milenkovic, N., M. Damjanovic, & M. Ristic, 2005: Study of Heavy Metal Pollution in Sediments from the Iron Gate (Danube River), Serbia and Montenegro. Polish Journal of Environmental Studies, 14(6).

Misak, R. and S. H. Attia, 1983: On sand dunes of Sinai peninsula. 19th ann. Meet. Geol. Soc. of Egypt.

Mohamed, E. H., 1987: Mineralogical studies for some Quaternary sediments in northern Sinai. M. Sc. Thesis, IsmailiaUni.

Nofal, A.M., S.Z. El Tawil, and F.H. Aly, 1980: Mise en valuer de la magnetite titanifere de gisements de sable cotier due Delta d'Egypte. Industrie Mineral les Techniques, (80) 203.

Omar, M.B., C. Mendiguchia, H. Er-Raioui, M. Marhraoui, G.H. Lafraoui, M.K.Ouladbdellah, M. Garcia-Vargas, & C. Moreno, 2015: Distribution of trace metals in marine sediments of Tetouan coast (North of Morocco): natural and anthropogenic sources. Environ. Earth Sci. (74) 4171- 4418.

Ramakrishan, C., R. Mani, and D.S.S. Babu, 1997: Ilmenite from the Chavara deposite, India: a critical evaluation. Mineral. Mag.,(61), 233-242.

Rittman, A. and F. M. Nakhla, 1958: Contribution to the study of Egyptian black sands. Egypt. Jour. Chem. (1) 127-135.

Rous, J. D. 1986: Garnet. Butterworth & Co. Ltd. 20-33.

Rozendaal, A. and C. Philander, 2000: Mineralogy of heavy mineral placers along the west coast of South Africa.- in: RAMMLMAIR, D., MEDERER, J., OBERTHÜR, T., HEIMANN, R. B. & PENTINGHAUS, H. (eds): Applied mineralogy in research, economy, technology, ecology and culture.- Proc. 6th Intern. Congr. on Applied Mineralogy, ICAM 2000, Göttingen, Germany, 17-19 July 2000: 417 – 420, 4 fig., 1 tab.; Rotterdam (Balkema).

Samir, A.M. 2000: The response of benthic foraminifera and ostracods to various pollution sources: a study from two lagoons in Egypt. J. Foraminifer. Res. (30) 83-98.

Selvaraj, K., V.R. Moha, & P. Szefer, 2004: Evaluation of metal contamination in coastal sediments of the Bay of Bengal, India: geochemical and statistical approaches. Mar. Pollut. Bull. (49)174-185

Shukri, N.M. 1950: The mineralogy of some Nile sediments. Quaternary Jour. Geol. Soc., London, (105) 511-534

Singer, P.C. 1977: Influence of dissolved organics on the distribution, transport and fate of heavy metals in aquatic system. In: Suffet, I.H. (Ed.), Fate of Pollutants in the Air and Water Environment, New York Part-1, 155-182.

Sinha, R. K. 1982: Industrial minerals. IBH publishing Co., Oxford, 480 p.

Soliman, S.M. 1964: Primary structure in a part of the Nile Delta sand beach. Development in Sedimentary Petrology, El Sevier Publ. Co. Amsterdam, pp. 379 - 390. Soliman, S.M. (1964): Primary structure in a part of the Nile Delta sand beach. Development in Sedimentary Petrology, El Sevier Publ. Co. Amsterdam, 379 - 390.

Temple, A.K. 1966: Alteration of ilmenite. Econ. Geol., (61) 695-714.

Teufer, G. and A.K. Temple, 1966: Pseudorutile - a new mineral intermediate between ilmenite and rutile in the alteration of ilmenite. Nature, (211)179-181.

Tourre, J.M. 1999: Rare earths: Recent market trends. Industrial Minerals, January, 37-43.

Van Emden, B., M. R., Thornber, J. Graham, and F.J . Lincoln, 1997: The incorporation of actinides in monazite and xenotime from placer deposits in Western Australia.- The Canadian Mineralogist, 35: 95 – 104, 5 fig., 4 tab.; Ottawa, ON.

Wang, W. X., Q. L. Yan, W. Fan, & Y. Xu, 2002: Bioavailability of sedimentary metals from a contaminated bay. Marine Ecology Progress Series (240) 27-38.

Wassef, S.N. and M.A. Mikhail, 1981: Distribution and mineralogy of ilmenite and other accessory minerals in the beach sands of west Rosetta, Egypt. Desert Instit. Bull., A.R.E.,(31) No.1-2,.17-29.

Zaghloul and Kamel, 1965 Z. M. Zaghloul, and K. E. Kamel, 1966: Mineralogical and petrographical features of zircon of black sands of Rosetta. Bull. Inst, Desert, de Egypte,(17) 1-17.

Zahran, M. A. E. K., Y. A. El-Amier, A. A. Elnaggar, H. A. E. A. Mohamed, & M. A. E. H. El-Alfy, 2015: Assessment and distribution of heavy metals pollutants in Manzala Lake, Egypt. Journal of Geoscience and Environment Protection 3(06), 107-122.